PAH growth in flames and space: phenalenyl radical from acenaphthylene

Zachariah D. Levey,[†] Benjamin A. Laws,[†] Srivathsan P. Sundar,[‡] Klaas Nauta,[†] Scott H. Kable,[†] Gabriel da Silva,[‡] John F. Stanton,[¶] and Timothy W. Schmidt[*,§]

[†]School of Chemistry, University of New South Wales, Sydney NSW 2052, Australia

[‡]Department of Chemical Engineering, The University of Melbourne, Parkville 3010, Australia

[¶]Department of Chemistry, University of Florida, Gainesville, Florida 32611, USA

[§]Centre of Excellence in Exciton Science, University of New South Wales, Sydney NSW 2052, Australia

E-mail: timothy.schmidt@unsw.edu.au

Abstract

Polycyclic aromatic hydrocarbons (PAHs) are intermediates in the formation of soot particles and interstellar grains. However, their formation mechanisms in combustion and interstellar environments are not fully understood. The production of tricyclic PAHs and, in particular, the conversion of a PAH containing a five-membered ring to one with a six-membered ring is of interest to explain PAH abundances in combustion processes. In the present work, resonant ionization mass spectrometry in conjunction with isotopic labelling is used to investigate the formation of the phenalenyl radical from acenaphthylene and methane in an electrical discharge. We show that in this environment, the CH cycloaddition mechanism converts a five-membered ring to a six-membered ring. This mechanism can occur in tandem with other PAH forma-

tion mechanisms such as hydrogen abstraction/ acetylene addition (HACA) to produce larger PAHs in flames and the interstellar medium.

Introduction

Polycyclic aromatic hydrocarbons (PAHs) are early intermediates in the soot formation process in both terrestrial[1–3] and interstellar environments.[4–7] Soot and PAHs formed during the incomplete combustion of fossil fuels are detrimental to human health due to their toxic and carcinogenic properties.[8–11] A ubiquitous existence of PAHs in the interstellar medium (ISM) is inferred from the aromatic infrared bands (AIBs), a set of infrared emission features between $3 - 20\,\mu$m that are characteristic of large PAH molecules.[12,13] It is thought that PAHs may comprise up to 20% of the total cosmic carbon abundance.[14–16] Benzene and benzonitrile, as well as fullerenes have been identified in the ISM.[17–20] However, there has not yet been a detection of any specific PAH.

The formation mechanism for interstellar PAHs is ambiguous. Astrochemical models of PAH formation are derived from combustion chemistry models.[21] Bottom-up molecular growth processes in circumstellar envelopes of carbon-rich stars are largely based on the hydrogen abstraction-acetylene addition (HACA) mechanism.[12] HACA proceeds by activation of a radical site by H-abstraction or addition, followed by addition of acetylene and ring closure.[22] It has been shown to occur for the formation of naphthalene from benzene via a phenylacetylene intermediate,[23,24] as well as for the formation of pyrene from 4-phenanthrenyl radical.[25]

However, there are some shortcomings of the HACA mechanism. Notably, modelling studies have reported that HACA under-predicts the concentration of PAHs in flames,[26] and under-predicts the PAH growth rate in astrochemical models.[27–29] To address these deficiencies, additional PAH formation mechanisms have been proposed. These include: recombination of resonance-stabilized radicals;[30–32] dimerization of small PAHs;[33] phenyl

addition/cyclization;[34] and methyl addition/cyclization.[35]

Acenaphthylene (ACYN) is considered the first island of stability pulling the HACA sequence forward.[36] Theoretical investigations of the reaction between naphthalene and acetylene show predominant formation of ACYN over phenanthrene and anthracene. Rapid cyclization after the addition of a single acetylene adjacent to the bay region to form a five-membered ring occurs faster than the addition of a second acetylene, followed by cyclization to form a third aromatic ring.[37] Indeed, three-quarters of the PAH products of the reaction contain a five-membered ring and less than 6% are PAHs with exclusively six-membered rings.[37] Hence, a mechanism to convert a five-membered ring on the edge of a PAH to a six-membered ring is necessary to account for pathways to larger PAHs.

Ring expansion has been proposed to take place by methylation followed by rearrangement and H-loss, and this mechanism has been invoked to account for benzene formation from cyclopentadienyl radical and naphthalene formation from indene.[30,38–43] Recently, calculations for the reaction of 1-acenaphthyl and methyl suggest that ring expansion of the five-membered ring occurs by methylation to produce 1H-phenalene and the phenalenyl radical.[44] The later[45,46] is posited to play a role in soot inception and growth.[32] It consists of three aromatic rings which share a central carbon atom. The gas phase excitation spectrum for the $D_1 \leftarrow D_0$ electronic transition was reported by our group.[47]

Additionally, expansion of a five-membered ring to a six-membered ring has been demonstrated through the reaction of pyrrole with the methylidyne radical (CH) to form pyridine,[48] and the reaction of cyclopentadiene with CH to form benzene.[49] CH in its ground state has been detected in combustion environments,[50–52] the interstellar medium[53,54] and under plasma conditions.[55] Reactions between CH and small unsaturated hydrocarbons and carbonyls can result in CH insertion to a π-bond through a cyclic intermediate (cycloaddition) followed by ring-opening.[49,56–59] This reaction has a negligible activation barrier, resulting in fast reaction rates. Isotopomer distribution experiments provide additional evidence for this mechanism through the reaction of CD with ethylene and pyrrole.[48,56]

In an electrical discharge containing methane, both methyl radicals and CH will be present. Introducing ACYN thus allows the CH insertion reaction to compete with the methylation ring expansion reaction to generate phenalenyl radicals. But, these mechanisms will incorporate a different number of deuterium atoms if CH_4 is substituted with CD_4. In this work, we investigated the products of an electrical discharge containing methane and ACYN. We identified phenalenyl radical ($C_{13}H_9$) as a product, and with perdeuterated methane detected a $C_{13}H_8D$ radical identified to be d1-phenalenyl. No $C_{13}H_7D_2$ radical was observed, which is strong evidence for CH cycloaddition as the dominant ring expansion mechanism. We propose that this reaction occurs in partnership with HACA to overcome the acenaphthylene bottleneck and lead to the generation of large PAHs.

Results and Discussion

The mass spectrum of an ACYN-containing argon beam (1% CH_4/ 99% Ar, Coregas) ionized by a 266 nm laser pulse is shown in Figure. 1a. At this wavelength, species with an $IE < 9.32$ eV may be ionized through (resonant) 2-photon ionization (R2PI). The ACYN parent signal (m/z 152) is minor compared to m/z 154. The m/z 154 signal corresponds to acenaphthene (ACN), an impurity in the sample, that is resonance-enhanced at 266 nm ($S_2 \leftarrow S_0$ electronic transition).[60] Peaks at m/z 153 and m/z 155 are assigned to hydrogen atom loss and the ^{13}C isotopologue of ACN, respectively. The species at m/z 172 is unidentified.

Figure 1b shows the mass spectrum from ACYN, with a high voltage (HV) discharge of -1.05 kV striking the molecular beam expansion 2 cm after the pulsed nozzle. Two new groups of ions are generated by the HV discharge between m/z 164 – 170 and m/z 178 – 184, respectively. These two groups are subsequently spaced from the parent signal (m/z 152) by 12 – 18 amu indicating the consecutive net addition of CH_n, where $n = 0 - 6$.

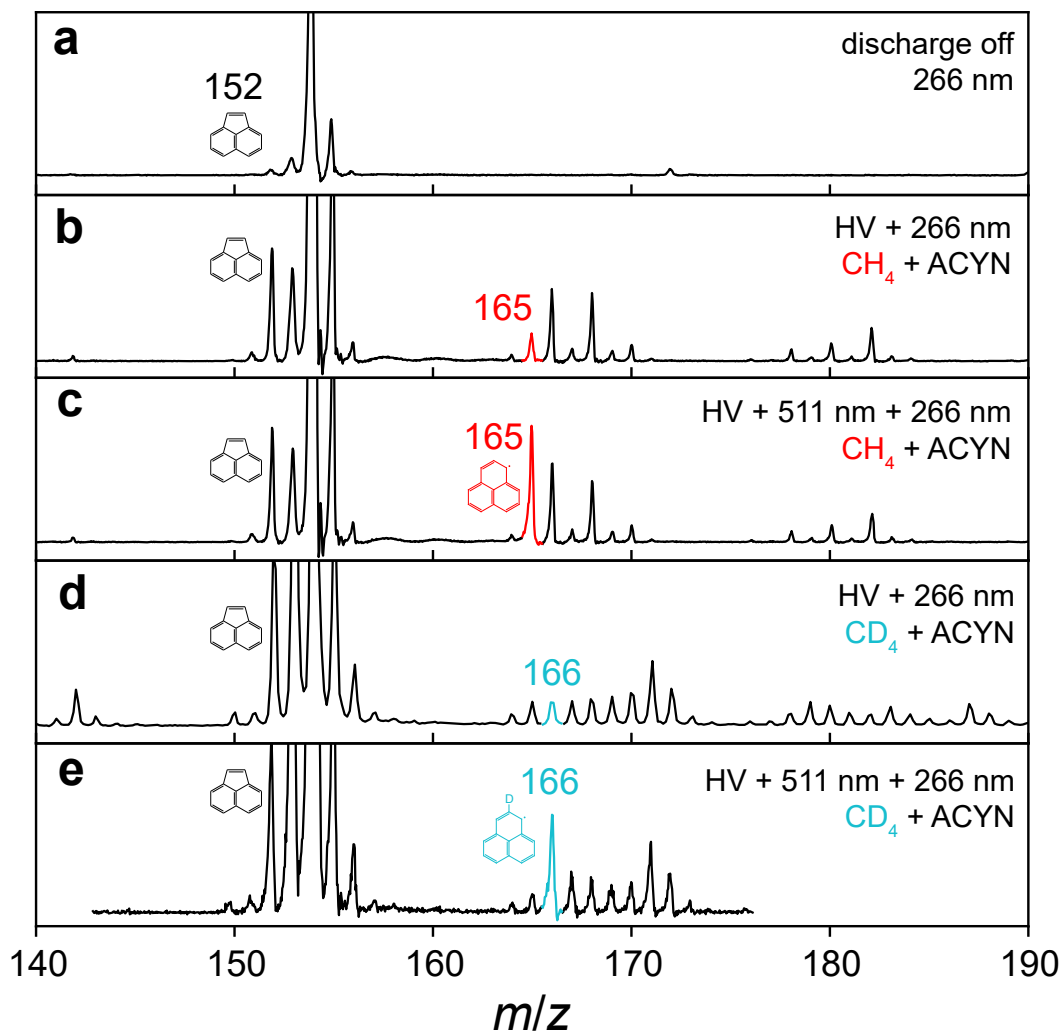The species at m/z 165 is assigned to the phenalenyl radical, $C_{13}H_9$, resulting from net

Figure 1: Mass spectra of products formed in high voltage (HV) electric discharge containing acenaphthylene and CH_4/CD_4. The phenalenyl radical (m/z 165) is highlighted in red. a) R2PI of ACYN at 266 nm without electric discharge. b) R2PI of products formed in electric discharge from ACYN + CH_4 at 266 nm. c) R2C2PI of products formed in electrical discharge from ACYN + CH_4. Excitation laser tuned to transition of phenalenyl at 19560 cm^{-1} (511 nm) and preceding ionisation laser at 266 nm by 30 ns. d) R2PI of products formed in electric discharge from ACYN + CD_4 at 266 nm. e) R2C2PI of products formed in electrical discharge from ACYN + CD_4. Excitation laser tuned to transition at 19565 cm^{-1} and preceding ionisation laser at 266 nm by 30 ns. The 1d-phenalenyl radical (m/z 166) is highlighted in cyan.

CH addition to ACYN. The peak at m/z 166 is assigned to 1H-phenalene, $C_{13}H_{10}$.[46] The other significant ion signal in this cluster is at m/z 168, which corresponds to the addition of CH_4 to ACYN, resulting in a molecular formula of $C_{13}H_{12}$. Additional minor peaks at

5

m/z 167 and 169 are most likely a combination of ^{13}C isotopologues (of m/z 166 and 168) and radical species.

To confirm the assignment of m/z 165, a tunable laser pulse was introduced to excite the radicals, preceding the ionizing laser pulse by ~ 30 ns. The wavelength of the excitation laser was scanned from $541 - 476$ nm to measure the resonant 2-colour 2-photon ionisation (R2C2PI) spectrum for the $D_1 \leftarrow D_0$ transition of the phenalenyl radical. Figure 2 shows a comparison with the R2C2PI spectrum recorded by O'Connor et al.[47] The resonance-enhanced ion signal resulting from the excitation laser being tuned to the wavelength of the strongest vibronic transition is shown in Figure 1c.
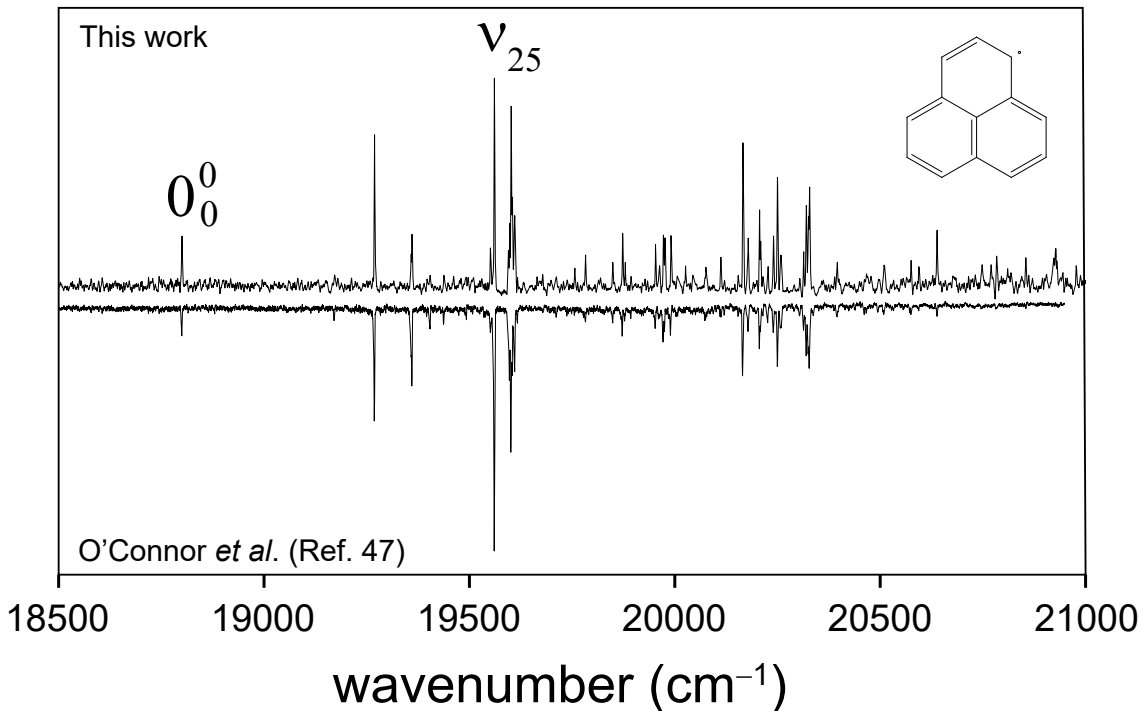

Figure 2: Resonant ionisation spectra of the phenalenyl radical (m/z 165). Top panel: R2C2PI spectrum recorded in this work (black). Bottom panel: R2C2PI spectrum recorded by O'Connor *et al.*[47] (blue).

The formation mechanism of the phenalenyl radical from ACYN was investigated by substituting perdeuterated methane, CD_4, into the seeding gas mixture. The resultant mass spectrum from 266 nm ionization is shown in Figure 1d. As with the non-deuterated mass spectrum, there are two distinct mass peak clusters produced by CD_n and C_2D_n addition to

ACYN and ACN.

The wavelength of the excitation laser was scanned around $511\,\text{nm}$ to maximize the m/z 166 signal. The resultant mass spectrum is displayed in Figure 1e. The resonance enhancement strongly suggests that the m/z 166 mass signal corresponds to the d1-phenalenyl radical, $C_{13}H_8D$.

To confirm this assignment, the excitation laser was scanned from $535\,\text{nm}$ to $475\,\text{nm}$. A comparison between the R2C2PI spectra of the phenalenyl radical and the species with m/z 166 is shown in Figure 3. Importantly, no other species produced a vibronic spectrum in this wavelength range. The strong resemblance to the spectrum of the phenalenyl radical confirms the assignment of m/z 166 to $C_{13}H_8D$. Each peak (cluster) in the deuterated spectrum has been shifted to higher energy by $\sim 5\,\text{cm}^{-1}$ compared to the original spectrum.

It may be tempting to ascribe the splitting of the origin peak at 18800 cm^{-1} to two different deuteration sites: either on or off the C_2 axes. However, the D_1 state of phenalenyl is a $E'' \otimes e'$ Jahn-Teller problem. Briefly, the potential energy part of the Hamiltonian for the $1E''$ state of phenalenyl can be written, in the diabatic basis,

$$
\mathbf{V} = \begin{bmatrix} \lambda\rho^2 - kQ_x + (\delta Q_x) & +kQ_y \\ +kQ_y & \lambda\rho^2 + kQ_x \end{bmatrix} \tag{1}
$$

where the rows and columns represent the two components of the degenerate electronic state, $|\mathcal{E}_x\rangle, |\mathcal{E}_y\rangle$. The symbols Q_x and Q_y are the components of a degenerate e' Jahn-Teller active mode, with $\rho^2 = Q_x^2 + Q_y^2$. The term in parentheses is discussed below. Diagonalization of this matrix $(\delta = 0)$ generates the familiar Jahn-Teller conical intersection.

With a single deuterium atom in the 2-position (C_{2v}), there will be a zero-point energy difference between positive and negative distortions in, say, Q_x. This is quantum-induced symmetry-breaking, as observed in dihydroanthracenyl radicals.[61] This effect is introduced by augmenting the linear term in at least one of the diagonal matrix elements. This tilts the potential to localize the minimum energy.[62] A full account of this effect in asymmetrically

deuterated cyclopentadienyl radicals is given in Reference 62.

In the basis of $|\mathcal{E}_{x,y}\rangle \otimes |v_x, v_y\rangle$ harmonic oscillator wavefunctions, $|\mathcal{E}_{x,y}\rangle \otimes \{|0, 0\rangle, |0, 1\rangle, |1, 0\rangle\}$ which are eigenfunctions of the potential $V = \lambda\rho^2$, with eigenvalues $\{\epsilon_0, \epsilon_1, \epsilon_1\}$

$$
\mathbf{H} = \begin{bmatrix}
\epsilon_0 & -k' & 0 & 0 & 0 & +k \\
-k' & \epsilon_1 & 0 & 0 & 0 & 0 \\
0 & 0 & \epsilon_1 & +k & 0 & 0 \\
0 & 0 & +k & \epsilon_0 & +k & 0 \\
0 & 0 & 0 & +k & \epsilon_1 & 0 \\
+k & 0 & 0 & 0 & 0 & \epsilon_1
\end{bmatrix}
\tag{2}
$$

where $\langle 1|Q_{x,y}|0\rangle = 1$ and $k' = k - \delta$. In the absence of zero-point energy effects, diagonalization of this matrix yields a degenerate ground state. However, the term δ lifts this degeneracy, resulting in a splitting, consistent with the experimental spectrum presented in Figure 3. An even more complicated pattern than is observed might be expected were there both isotopomers present, in addition to the asymmetric Jahn-Teller effect. A complete assignment of the deuterated spectrum will be provided in a forthcoming publication.

This result provides insight into the formation mechanism of phenalenyl radical from ACYN. A mass shift from m/z 165 to 166 shows that only a single deuterium atom has been substituted into the phenalenyl radical. This is inconsistent with the methylation mechanism put forth by Porfiriev $et.$ $al.$,[44] in which hydrogen abstraction from ACYN allows for CH_3 (CD_3) addition to the resultant radical site of the acenaphthyl radical. The methylated product may then follow several different pathways leading to the phenalenyl radical. However, each pathway in their proposed reaction scheme involves two hydrogen (deuterium) atoms from the CH_3 (CD_3) radical being present in the final product.[44] The deuterated reaction scheme for the methylation mechanism is shown in Figure 4a.

Results from this work are in agreement with the CH cycloaddition mechanism reported by Trevitt and Goulay,[59] where CH addition across a double bond allows for expansion of the
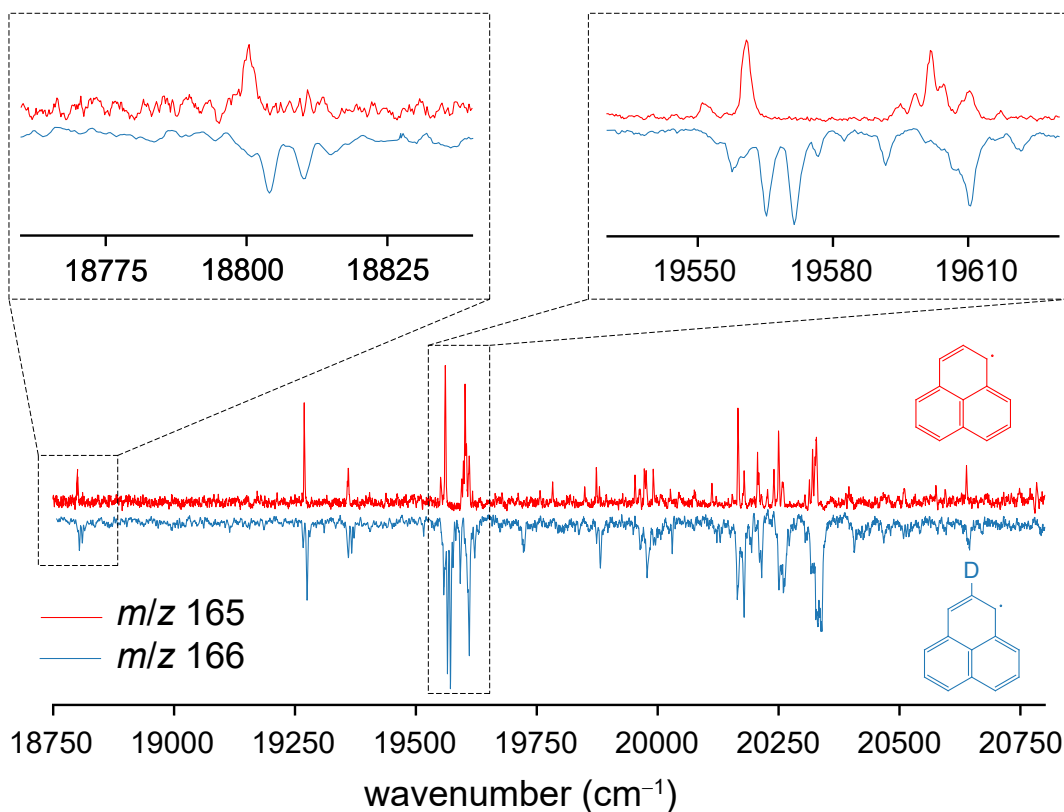
Figure 3: Top: A comparison of the resonant ionisation spectra of phenalenyl radical ($C_{13}H_9$) (red) and deuterated phenalenyl radical ($C_{13}H_8D$) (blue). Top left: Origin band. Top right: Most intense bands in the spectrum.

five-membered ring in ACYN to form one of the six-membered rings in phenalenyl. However, this process is also complicated by the potential for CH reaction at the six-membered rings in ACYN, which one might expect to lead to tropyl- and benzyl-like structures. To investigate these aspects of the mechanism, we carried out a computational chemistry investigation.

Figure 5 shows the reaction scheme developed for phenalenyl formation from CH attack on the five-membered ACYN ring. The cycloadduct channel, depicted as the lower pathway, is formed via CH attack across the double bond of the five-membered ring and cuts through multiple pathways to directly form phenalenyl. By tracing the single added hydrogen (deuterium) along this pathway we can deduce it will finish in the 2-position (C2v). CH insertion into the C-H bond of the five-membered ACYN ring may also occur. The resultant intermediate undergoes ring opening chemistry, generating phenalenyl either via a cycloadduct,
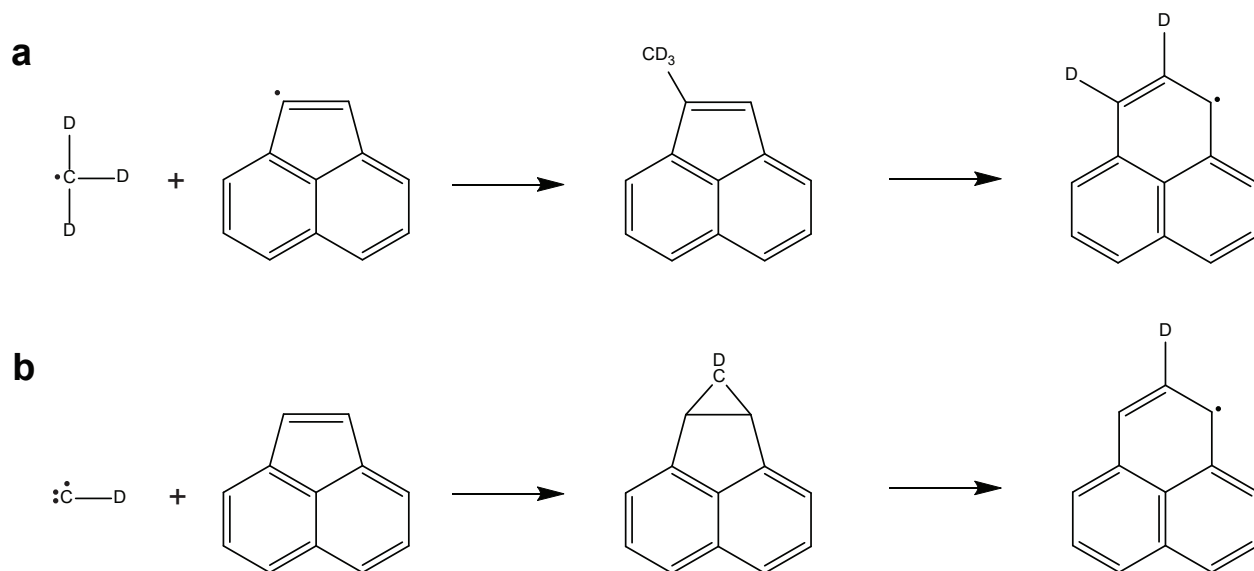
9

Figure 4: a) Methylation reaction scheme for formation of phenalenyl radical from 1-acenaphthyl radical + $CD_3\cdot$, proposed by Porfiriev *et. al.*[44] b) Cycloaddition reaction scheme for the formation of phenalenyl radical from acenaphthylene + CD·.

or by direct insertion into the double bond. Tracing the hydrogen (deuterium) along these pathways results in an ambiguous final position, either on or off the C2 axes. However, as only one isotopomer appears to be present in the experimental spectra presented in Figure 3, the reaction mechanism must have a propensity to favour one isotopomer over the other.

As mentioned, CH reaction with ACYN may also proceed via attack at a six-membered ring, where cycloaddition and C-H bond insertion are again both available. Figure 6 demonstrates that the cycloaddition process leads to a tropyl-like intermediate structure with no barrier. It may then rearrange to phenalenyl, with all barriers well below entrance. The formed tropyl-like intermediate undergoes an internal H-atom transfer, a rate limiting step in the rearrangement to phenalenyl. Subsequently, a ring formation and cleavage mechanism occurs via a low energy barrier to finally produce phenalenyl. The C-H bond insertion mechanism is somewhat more complex, as there are three unique H atoms on the six-membered rings, leading to three unique benzyl-like intermediates. One of these three processes is illustrated in Figure 7 with the others presented in the supplementary information. Again, formation of the initial resonantly stabilised radical (RSR) is barrierless and highly exother-
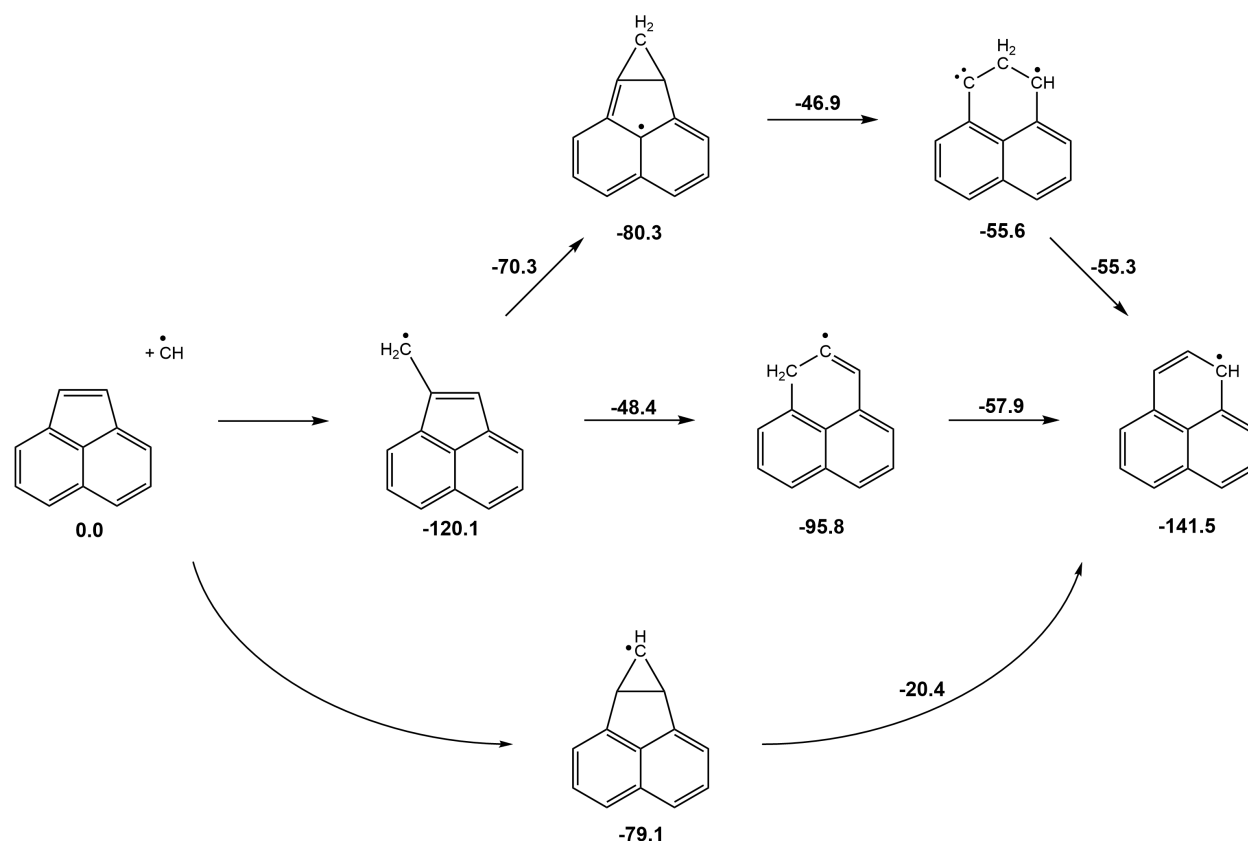
Figure 5: Reaction scheme for formation of phenalenyl from a CH attack on the five-membered ACYN ring. Calculations were performed at MO6-2X/6-31G(2df,p) level of theory. The energies are in kcal/mol.

mic, providing it with significant excess vibrational energy to overcome subsequent barriers to rearrangement. Here this occurs via CH_2 attack followed by insertion into the ring at either of the two adjacent carbons. A subsequent H-shift then returns the tropyl-like structure seen before, which will follow on to produce phenalenyl.

In short, all roads lead to phenalenyl. The most straightforward route is via direct attack at the five-membered ring. Cycloaddition and insertion make other RSRs, but in low pressure and energetic environments they will be able to rearrange to phenalenyl.

The CH cycloaddition mechanism working in conjunction with the HACA mechanism is a plausible explanation for the production of the multitude of large, planar PAHs formed in combustion processes. The HACA mechanism will predominantly generate a five-membered ring in the bay region of a PAH. The CH cycloaddition mechanism will then cause ring expan-
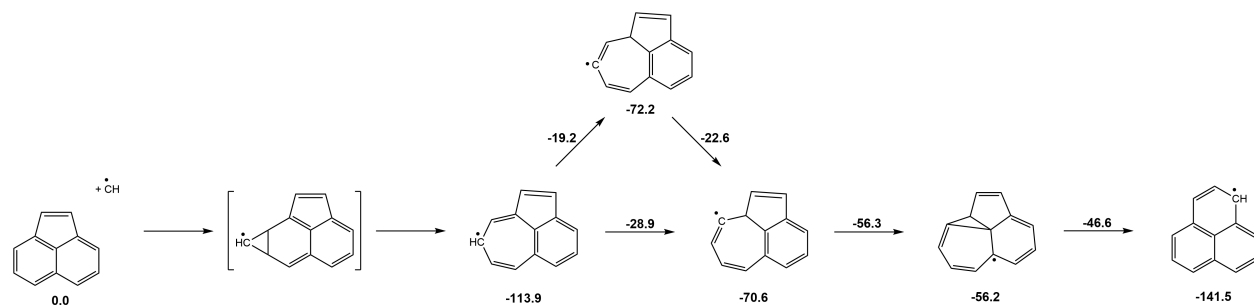
Figure 6: Formation of phenalenyl from a CH attack on the 6-membered ACYN ring, via a tropyl-like intermediate RSR. Calculations were performed at MO6-2X/6-31G(2df,p) level of theory. The energies are in kcal/mol.
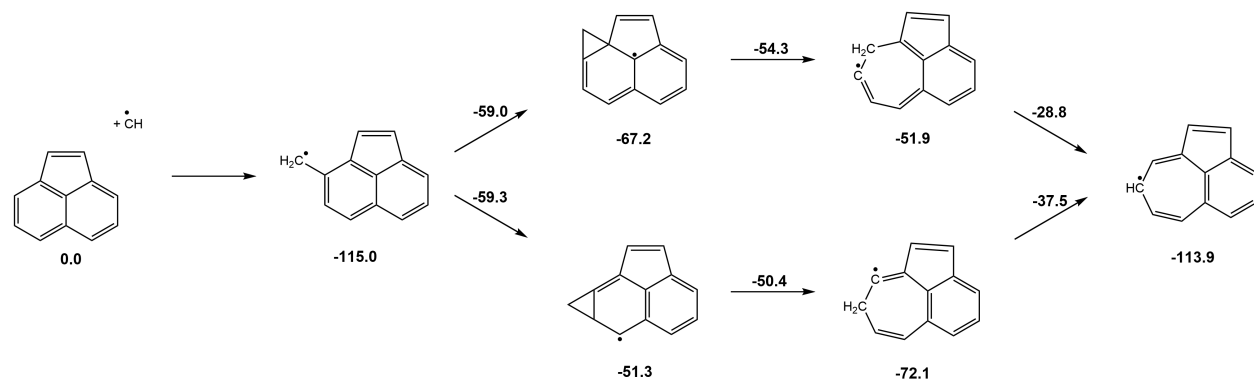

Figure 7: Reaction scheme for CH insertion, forming the tropyl-like RSR. Calculations were performed at MO6-2X/6-31G(2df,p) level of theory. The energies are in kcal/mol.

sion to form another six-membered ring, and the process can repeat itself. This subsequent combination of mechanisms can account for the formation of PAHs beyond the phenalenyl radical, such as pyrene, cyclopenta[cd]pyrene and the olympicenyl radical. The high concentrations of CH radicals in combustion environments and its detection in the interstellar medium further supports the plausibility of CH cycloaddition as a crucial component of the PAH formation mechanism.[50–54]

Conclusion

We have shown that the phenalenyl radical is produced as a discharge product of ACYN and methane. Substituting CD_4 into the seeding gas mixture indicated that the dominant formation mechanism was CH cycloaddition. Calculations show that this reaction occurs

12

through the insertion of CH across the C−C π-bond of the cyclopenta-fused ring of ACYN, forming a three-membered ring, followed by ring-opening to generate the phenalenyl radical. This contradicts the suggestion that the reaction occurs by methylation.[44] The conversion of ACYN to the phenalenyl radical is an example of a five-membered ring expanding to a six-membered ring, which is of importance in combustion and interstellar chemistry, and the abundance of CH supports the proposed mechanism in these environments. The CH cycloaddition mechanism may work in tandem with the HACA mechanism to generate larger PAHs beyond the tricyclic phenalenyl radical.

Experimental Details

The apparatus used for R2C2PI and R2PI has been described previously in more detail.[63] A sample of ACYN is heated to 85°C and seeded in 5 bar of a methane/argon gas mixture(Coregas, 1% Methane/99% Argon). The seeded gas mix is expanded into a differentially pumped vacuum chamber through a pulsed discharge nozzle (PDN). A voltage of −1.05kV is applied to the outer electrode of the PDN for 100 μs, resulting in a strike which coincides with the expanding gas pulse.

Methane is incorporated into the backing gas mixture to provide an additional source of CH. The discharge products are cooled through supersonic expansion and the central, coldest section of the molecular beam ($\sim$10K) is passed through a 2 mm diameter skimmer into a second differentially pumped chamber. The cold molecular beam is probed between two positively charged extraction plates of a Wiley-McLaren-type time-of-flight mass spectrometer (ToF-MS) using R2C2PI spectroscopy.

A Nd:YAG-pumped dye laser is used as an excitation laser to investigate the first electronic excited states of the phenalenyl radical. The excited radicals are subsequently ionized using the fourth harmonic (266 nm) of a second Nd:YAG laser, pulsing a few tens of nanoseconds after the excitation pulse. The resultant cations are orthogonally accelerated up the

length of the ToF-MS and detected by a multichannel plate (MCP) which produces an electronic signal that is displayed on an oscilloscope. Custom-written LabView software is used to record the spectra and a wavemeter is used to calibrate the laser wavelengths.

Computational details

Quantum chemical computations were performed using Gaussian-16 program.[64] MO62-X / 6- 31G(2df,p) level of theory and G3X-K were utilized to perform geometry optimizations and single point energies respectively. G3X-K predicts energies accurately within 0.6 kcal/mol, appropriate for thermochemical kinetics.[65] Frequency computations verified that all stationary points possess zero imaginary frequencies and one for all saddle points. Intrinsic reaction co-ordinate calculations confirm the connectivity of transition states.

Acknowledgement

References

(1) Frenklach, M. Reaction mechanism of soot formation in flames. *Phys. Chem. Chem. Phys.* **2002**, *4*, 2028–2037.

(2) Wang, H. Formation of nascent soot and other condensed-phase materials in flames. *P. Combust. Inst.* **2011**, *33*, 41 – 67.

(3) Faccinetto, A.; Irimiea, C.; Minutolo, P.; Commodo, M.; D'Anna, A.; Nuns, N.; Carpentier, Y.; Pirim, C.; Desgroux, P.; Focsa, C.; et al., Evidence on the formation of

dimers of polycyclic aromatic hydrocarbons in a laminar diffusion flame. *Commun. Chem.* **2020**, *3*, 112.

(4) Henning, T.; Salama, F. Carbon in the Universe. *Science* **1998**, *282*, 2204–2210.

(5) Jäger, C.; Huisken, F.; Mutschke, H.; Jansa, I. L.; Henning, T. Formation of Polycyclic Aromatic Hydrocarbons and Carbonaceous Solids in Gas-Phase Condensation Experiments. *Astrophys. J.* **2009**, *696*, 706–712.

(6) Draine, B. T.; Li, A. Infrared Emission from Interstellar Dust. I. Stochastic Heating of Small Grains. *Astrophys. J.* **2001**, *551*, 807–824.

(7) Draine, B. T.; Li, A. Infrared Emission from Interstellar Dust. IV. The Silicate-Graphite-PAH Model in the Post-Spitzer Era. *Astrophys. J.* **2007**, *657*, 810–837.

(8) Ramanathan, V.; Carmichael, G. Global and regional climate changes due to black carbon. *Nat. Geosci.* **2008**, *1*, 221–227.

(9) Finlayson-Pitts, B. J. Tropospheric Air Pollution: Ozone, Airborne Toxics, Polycyclic Aromatic Hydrocarbons, and Particles. *Science* **1997**, *276*, 1045–1051.

(10) Denissenko, M. F.; Pao, A.; Tang, M.-S.; Pfeifer, G. P. Preferential Formation of Benzo[a]pyrene Adducts at Lung Cancer Mutational Hotspots in P53. *Science* **1996**, *274*, 430–432.

(11) Tiwari, M.; Sahu, S.; Pandit, G. Distribution of PAHs in different compartment of creek ecosystem: Ecotoxicological concern and human health risk. *Environ. Toxicol. Phar.* **2017**, *50*, 58 – 66.

(12) Tielens, A. G. G. M. The molecular universe. *Rev. Mod. Phys.* **2013**, *85*, 1021–1081.

(13) Pech, C.; Joblin, C.; Boissel, P. The profiles of the aromatic infrared bands explained with molecular carriers. *Astron. Astrophys.* **2002**, *388*, 639–651.

(14) Tielens, A. Interstellar Polycyclic Aromatic Hydrocarbon Molecules. *Annu. Rev. Astron. Astr.* **2008**, *46*, 289–337.

(15) Dwek, E.; Arendt, R. G.; Fixsen, D. J.; Sodroski, T. J.; Odegard, N.; Weiland, J. L.; Reach, W. T.; Hauser, M. G.; Kelsall, T.; Moseley, S. H.; et al., Detection and Characterization of Cold Interstellar Dust and Polycyclic Aromatic Hydrocarbon Emission, from COBE Observations. *Astrophys. J.* **1997**, *475*, 565–579.

(16) D'Hendecourt, L.; Ehrenfreund, P. Spectroscopic properties of polycyclic aromatic hydrocarbons (PAHs) and astrophysical implications. *Adv. Space Res.* **1997**, *19*, 1023–1032.

(17) Cernicharo, J.; Heras, A. M.; Tielens, A. G. G. M.; Pardo, J. R.; Herpin, F.; Guélin, M.; Waters, L. B. F. M. *Infrared Space Observatory's* Discovery of C_4H_2, C_6H_2, and Benzene in CRL 618. *Astrophys. J.* **2001**, *546*, L123–L126.

(18) McGuire, B. A.; Burkhardt, A. M.; Kalenskii, S.; Shingledecker, C. N.; Remijan, A. J.; Herbst, E.; McCarthy, M. C. Detection of the aromatic molecule benzonitrile (c-C_6H_5CN) in the interstellar medium. *Science* **2018**, *359*, 202–205.

(19) Cami, J.; Bernard-Salas, J.; Peeters, E.; Malek, S. E. Detection of C_{60} and C_{70} in a Young Planetary Nebula. *Science* **2010**, *329*, 1180–1182.

(20) Campbell, E. K.; Holz, M.; Gerlich, D.; Maier, J. P. Laboratory confirmation of C_{60}^+ as the carrier of two diffuse interstellar bands. *Nature* **2015**, *523*, 322–323.

(21) Frenklach, M.; Feigelson, E. D. Formation of Polycyclic Aromatic Hydrocarbons in Circumstellar Envelopes. *Astrophys. J.* **1989**, *341*, 372.

(22) Frenklach, M.; Clary, D. W.; Gardiner, W. C.; Stein, S. E. Detailed kinetic modeling of soot formation in shock-tube pyrolysis of acetylene. *Symp. (Int.) Combust.* **1985**, *20*, 887 – 901.

(23) Parker, D. S. N.; Kaiser, R. I.; Troy, T. P.; Ahmed, M. Hydrogen Abstraction/Acetylene Addition Revealed. *Angew. Chem. Int. Edit.* **2014**, *53*, 7740–7744.

(24) Yang, T.; Troy, T. P.; Xu, B.; Kostko, O.; Ahmed, M.; Mebel, A. M.; Kaiser, R. I. Hydrogen-Abstraction/Acetylene-Addition Exposed. *Angew. Chem. Int. Edit.* **2016**, *55*, 14983–14987.

(25) Zhao, L.; Kaiser, R. I.; Xu, B.; Ablikim, U.; Ahmed, M.; Joshi, D.; Veber, G.; Fischer, F. R.; Mebel, A. M. Pyrene synthesis in circumstellar envelopes and its role in the formation of 2D nanostructures. *Nat. Astron.* **2018**, *2*, 413–419.

(26) Raj, A.; Prada, I. D. C.; Amer, A. A.; Chung, S. H. A reaction mechanism for gasoline surrogate fuels for large polycyclic aromatic hydrocarbons. *Combust. Flame* **2012**, *159*, 500 – 515.

(27) Micelotta, E. R.,; Jones, A. P.,; Tielens, A. G. G. M., Polycyclic aromatic hydrocarbon processing in a hot gas. *Astron. Astrophys.* **2010**, *510*, A37.

(28) Micelotta, E. R.,; Jones, A. P.,; Tielens, A. G. G. M., Polycyclic aromatic hydrocarbon processing in interstellar shocks. *Astron. Astrophys.* **2010**, *510*, A36.

(29) Micelotta, E. R.,; Jones, A. P.,; Tielens, A. G. G. M., Polycyclic aromatic hydrocarbon processing by cosmic rays. *Astron. Astrophys.* **2011**, *526*, A52.

(30) Melius, C. F.; Colvin, M. E.; Marinov, N. M.; Pit, W. J.; Senkan, S. M. Reaction mechanisms in aromatic hydrocarbon formation involving the C_5H_5 cyclopentadienyl moiety. *Symp. (Int.) Combust.* **1996**, *26*, 685 – 692.

(31) Miller, J. A.; Melius, C. F. Kinetic and thermodynamic issues in the formation of aromatic compounds in flames of aliphatic fuels. *Combust. Flame* **1992**, *91*, 21 – 39.

(32) Johansson, K. O.; Head-Gordon, M. P.; Schrader, P. E.; Wilson, K. R.; Michelsen, H. A.

Resonance-stabilized hydrocarbon-radical chain reactions may explain soot inception and growth. *Science* **2018**, *361*, 997–1000.

(33) Siegmann, K.; Sattler, K. Formation mechanism for polycyclic aromatic hydrocarbons in methane flames. *J. Chem. Phys.* **2000**, *112*, 698–709.

(34) Shukla, B.; Susa, A.; Miyoshi, A.; Koshi, M. Role of Phenyl Radicals in the Growth of Polycyclic Aromatic Hydrocarbons. *J. Phys. Chem. A* **2008**, *112*, 2362–2369, PMID: 18298104.

(35) Shukla, B.; Miyoshi, A.; Koshi, M. Role of Methyl Radicals in the Growth of PAHs. *J. Am. Soc. Mass Spectr.* **2010**, *21*, 534 – 544.

(36) Frenklach, M.; Mebel, A. M. On the mechanism of soot nucleation. *Phys. Chem. Chem. Phys.* **2020**, *22*, 5314–5331.

(37) Kislov, V. V.; Sadovnikov, A. I.; Mebel, A. M. Formation Mechanism of Polycyclic Aromatic Hydrocarbons beyond the Second Aromatic Ring. *J. Phys. Chem. A* **2013**, *117*, 4794–4816, PMID: 23672431.

(38) Moskaleva, L.; Mebel, A.; Lin, M. The $CH_3+C_5H_5$ reaction: A potential source of benzene at high temperatures. *Symp. (Int.) Combust.* **1996**, *26*, 521 – 526.

(39) Sharma, S.; Green, W. H. Computed Rate Coefficients and Product Yields for c-C_5H_5 + CH_3 → Products. *J. Phys. Chem. A* **2009**, *113*, 8871–8882, PMID: 19591475.

(40) Mebel, A. M.; Georgievskii, Y.; Jasper, A. W.; Klippenstein, S. J. Pressure-dependent rate constants for PAH growth: formation of indene and its conversion to naphthalene. *Faraday Discuss.* **2016**, *195*, 637–670.

(41) Jasper, A. W.; Hansen, N. Hydrogen-assisted isomerizations of fulvene to benzene and of larger cyclic aromatic hydrocarbons. *P. Combust. Inst.* **2013**, *34*, 279 – 287.

(42) Zhao, L.; Kaiser, R. I.; Lu, W.; Xu, B.; Ahmed, M.; Morozov, A. N.; Mebel, A. M.; Howlader, A. H.; Wnuk, S. F. Molecular mass growth through ring expansion in polycyclic aromatic hydrocarbons via radical–radical reactions. *Nat. Commun.* **2019**, *10*.

(43) Mebel, A. M.; Landera, A.; Kaiser, R. I. Formation Mechanisms of Naphthalene and Indene: From the Interstellar Medium to Combustion Flames. *J. Phys. Chem. A* **2017**, *121*, 901–926.

(44) Porfiriev, D. P.; Azyazov, V. N.; Mebel, A. M. Conversion of acenaphthalene to phenalene via methylation: A theoretical study. *Combust. Flame* **2020**, *213*, 302 – 313.

(45) Morita, Y.; Suzuki, S.; Sato, K.; Takui, T. Synthetic organic spin chemistry for structurally well-defined open-shell graphene fragments. *Nat. Chem.* **2011**, *3*, 197–204.

(46) O'Connor, G. D.; Chan, B.; Sanelli, J. A.; Cergol, K. M.; Dryza, V.; Payne, R. J.; Bieske, E. J.; Radom, L.; Schmidt, T. W. Hydrogen-adduction to open-shell graphene fragments: spectroscopy, thermochemistry and astrochemistry. *Chem. Sci.* **2017**, *8*, 1186–1194.

(47) O'Connor, G. D.; Troy, T. P.; Roberts, D. A.; Chalyavi, N.; Fückel, B.; Crossley, M. J.; Nauta, K.; Stanton, J. F.; Schmidt, T. W. Spectroscopy of the Free Phenalenyl Radical. *J. Am. Chem. Soc.* **2011**, *133*, 14554–14557, PMID: 21854045.

(48) Soorkia, S.; Taatjes, C. A.; Osborn, D. L.; Selby, T. M.; Trevitt, A. J.; Wilson, K. R.; Leone, S. R. Direct detection of pyridine formation by the reaction of CH (CD) with pyrrole: a ring expansion reaction. *Phys. Chem. Chem. Phys.* **2010**, *12*, 8750.

(49) Caster, K. L.; Donnellan, Z. N.; Selby, T. M.; Goulay, F. Kinetic Investigations of the CH ($X^2\Pi$) Radical Reaction with Cyclopentadiene. *J. Phys. Chem. A* **2019**, *123*, 5692–5703, PMID: 31194547.

(50) Love, N.; Parthasarathy, R. N.; Gollahalli, S. R. Concentration Measurements of CH and OH Radicals in Laminar Biofuel Flames. *Int. J. Green Energy* **2011**, *8*, 113–120.

(51) Tinaut, F. V.; Reyes, M.; Giménez, B.; Pastor, J. V. Measurements of OH* and CH* Chemiluminescence in Premixed Flames in a Constant Volume Combustion Bomb under Autoignition Conditions. *Energ. Fuel* **2011**, *25*, 119–129.

(52) Zhang, T.; Guo, Q.; Liang, Q.; Dai, Z.; Yu, G. Distribution Characteristics of OH*, CH*, and C_2* Luminescence in CH_4/O_2 Co-flow Diffusion Flames. *Energ. Fuel* **2012**, *26*, 5503–5508.

(53) Gerin, M., et al. Interstellar CH absorption in the diffuse interstellar medium along the sight-lines to G10.6-0.4 (W31C), W49N, and W51. *Astron. Astrophys.* **2010**, *521*, L16.

(54) Adams, W. S. Some Results with the COUDÉ Spectrograph of the Mount Wilson Observatory. *Astrophys. J.* **1941**, *93*, 11.

(55) Zhou, J.; Fisher, E. R. Surface Reactivity and Energetics of CH Radicals during Plasma Deposition of Hydrogenated Diamondlike Carbon Films. *J. Phys. Chem. B* **2006**, *110*, 21911–21919, PMID: 17064158.

(56) Goulay, F.; Trevitt, A. J.; Meloni, G.; Selby, T. M.; Osborn, D. L.; Taatjes, C. A.; Vereecken, L.; Leone, S. R. Cyclic Versus Linear Isomers Produced by Reaction of the Methylidyne Radical (CH) with Small Unsaturated Hydrocarbons. *J. Am. Chem. Soc.* **2009**, *131*, 993–1005, PMID: 19123915.

(57) Trevitt, A. J.; Prendergast, M. B.; Goulay, F.; Savee, J. D.; Osborn, D. L.; Taatjes, C. A.; Leone, S. R. Product Branching Fractions of the CH + Propene Reaction from Synchrotron Photoionization Mass Spectrometry. *J. Phys. Chem. A* **2013**, *117*, 6450–6457.

(58) Goulay, F.; Trevitt, A. J.; Savee, J. D.; Bouwman, J.; Osborn, D. L.; Taatjes, C. A.; Wilson, K. R.; Leone, S. R. Product Detection of the CH Radical Reaction with Acetaldehyde. *J. Phys. Chem. A* **2012**, *116*, 6091–6106.

(59) Trevitt, A. J.; Goulay, F. Insights into gas-phase reaction mechanisms of small carbon radicals using isomer-resolved product detection. *Phys. Chem. Chem. Phys.* **2016**, *18*, 5867–5882.

(60) Swiderek, P.; Hohlneicher, G. Comment on the Low Lying Singlet States of Acenaphthene. *Ber. Bunsenges. Phys. Chem.* **1991**, *95*, 1683–1684.

(61) Krechkivska, O.; Wilcox, C. M.; Nauta, K.; Kable, S. H.; Schmidt, T. W. Quantum-Induced Symmetry Breaking in the Deuterated Dihydroanthracenyl Radical. *J. Phys. Chem. A* **2019**, *123*, 6711–6719.

(62) Yu, L.; Cullin, D. W.; Williamson, J. M.; Miller, T. A. High resolution laser spectroscopy of asymmetrically deuterated cyclopentadienyl radicals: A study of vibronic degeneracy resolution and Jahn–Teller distortion. *J. Chem. Phys.* **1993**, *98*, 2682–2698.

(63) Reilly, N. J.; Nakajima, M.; Troy, T. P.; Chalyavi, N.; Duncan, K. A.; Nauta, K.; Kable, S. H.; Schmidt, T. W. Spectroscopic Identification of the Resonance-Stabilized cis- and trans-1-Vinylpropargyl Radicals. *J. Am. Chem. Soc.* **2009**, *131*, 13423–13429.

(64) Frisch, M. J. et al. Gaussian~16 Revision C.01. 2016; Gaussian Inc. Wallingford CT.

(65) da Silva, G. G3X-K theory: A composite theoretical method for thermochemical kinetics. *Chemical Physics Letters* **2013**, *558*, 109–113.